IOP Conference Series: Earth and Environmental Science

PAPER • **OPEN ACCESS**

Formation of gases and aerosol composition in background and urban areas of Western Siberia: a case study for the record-breaking hot April of 2020

To cite this article: O Yu Antokhina *et al* 2020 *IOP Conf. Ser.: Earth Environ. Sci.* **611** 012035

View the article online for updates and enhancements.

This content was downloaded from IP address 109.227.215.184 on 22/12/2020 at 13:17

Formation of gases and aerosol composition in background and urban areas of Western Siberia: a case study for the record-breaking hot April of 2020

O Yu Antokhina[1], P N Antokhin[1], M Yu Arshinov[1], B D Belan[1], D K Davydov[1], A V Kozlov[1], D E Savkin[1], T K Sklyadneva[1], G N Tolmachev[1] abd A V Fofonov[1]

[1]V E Zuev Institute of Atmospheric Optics of the Siberian Branch of the Russian Academy of Sciences, 1, Academician Zuev square, Tomsk, Russia

olgayumarchenko@gmail.com

Abstract. This paper presents results of a comprehensive analysis of the formation of gases and aerosol composition during the anomalously hot April 2020 in Western Siberia. The analysis of the observed change in atmospheric composition and a modeling study with the WRF-Chem is carried out for suburban (TOR-station) and background (FON-station) areas. Two episodes of increased gases and aerosols were detected: 13-15 April with a peak on 14 (in most part for the TOR station: increased NO, NO_2, CO, CO_2, aerosols) and 17-24 April with a peak on 23 (for both stations O_3, aerosol, in most part for the FON station: NO_2, SO_2, CO, and CO_2). Atmospheric circulation in the first episode was characterized by mesoscale differences between the two studied locations (surface temperature delta, although both stations are in the same region of large-scale transfers). For the second episode, a large scale atmospheric ridge was observed,which caused a transboundary transfer from Northern Kazakhstan and early wildfires. The simulation with WRF has demonstrated in most cases only the role of wildfires and, in general, has not demonstrated any observed differences between the two episodes. It shows that there is a need to search for more sensitive methods of discovering sources of pollution.

1. Introduction

The study of changes in the gases and aerosol composition during the period of observed climatic changes is necessary. There are many feedbacks associated with the chemical composition of the atmosphere and climate system. One of the exciting aspects of this matter is the study of the influence of extreme episodes associated with atmospheric circulation and changes in surface temperature. April 2020 was the second abnormally hot (the first one was in 2016) for our planet. The global temperature anomaly was 1.06°C (April 2020: another month that was the second warmest on record, https://bit.ly/3hWwibW). The most pronounced temperature anomalies were characteristic of Western Siberia, where the average monthly temperature exceeded the norm by an average of 5°C, and in the northern regions of Western Siberia by 10-12°C. According to the Russian weather services departments for Western Siberia, April 2020 was the first hottest April (https://ria.ru/20200420/1570277368.html, https://bit.ly/2Z6Cabk).

In the present paper, first we discuss the changes observed in the gas and aerosol composition during an abnormally warm April, analyze the circulation patterns associated with the transfer of air

Content from this work may be used under the terms of the Creative Commons Attribution 3.0 licence. Any further distribution of this work must maintain attribution to the author(s) and the title of the work, journal citation and DOI.
Published under licence by IOP Publishing Ltd

masses, as well as the formation of atmospheric blocking conditions. The relevance of this study is connected both with the unusual weather conditions of April 2020 and with the fact that mainly the influence of circulation on the formation of the gas and aerosol composition of the atmosphere was considered for the winter and summer periods [1, 2], and to a lesser extent during the transitional seasons. In the second part of the paper, we compare the modeled with WRF-Chem data with the changes observed in the gas (CO, NO, NO_2, SO_2, O_3) and aerosol composition during the abnormally warm April. This allows us to make some conclusions about the quality of simulation for extremal conditions of background and suburban areas.

2. Data and methods

The gas and aerosol concentration for April 2020 was derived from the Tropospheric Ozone Research Station (TOR-station) [3] and Fonovaya Station (FON-station) [4]. The TOR and FON stations are located in suburban (Tomsk, 56°28'41"N, 85°03'15"E) and background areas (Kireyewsk, 56°21'50"N, 84°05'28" E), respectively. We used daily chemical composition and temperature data.

Atmospheric data used in this study are from the European Center for Medium-Range Weather Forecasts ECMWF Era 5 [5, 6] and NCEP/NCAR Reanalysis 1 [7]. The spatial and temporal resolution is 2.5°×2.5° and 12 UTC (0.75°×0.75° for potential temperature).

To clarify the period and position of blocking processes, we use a GHGS (geopotential height – gradient south) criterion developed in [8-10] (equation 1). We use the GHGS with the fix blocking latitude (φ_{fix}) and flexible blocking latitude (φ_{flex}) based on [11],

$$GHGS = \frac{Z(\varphi_0)-Z(\varphi_s)}{\varphi_0-\varphi_s}, \quad 1$$

where Z is the 500 hPa geopotential height, for φ_{fix}: φ_0=60° N ±Δ, φ_s=40° N ±Δ, for φ_{flex}= φ_0=70° N ±Δ, φ_s=50° N ±Δ (for Western Siberia).

Unlike [8, 9], we took the following values for Δ: -5°, -2.5°, 0°, 2.5°, or 5°, which were first offered in [10]. To clarify the blocking dates, we also used the potential temperature on the dynamic tropopause (PV–θ). According to [12], PV–θ is a perfect candidate for studying the development of blocking since it is materially conserved in time, providing an excellent tracer for the air masses contributing to blocking formation, and can be inverted to give a balanced component of the flow. Also, the reversal of the meridional gradient PV–θ is associated with Rossby wave-breaking [12].

To analyze the general direction of air masses, we utilized the HYSPLIT model (https://www.ready.noaa.gov/HYSPLIT.php). We used daily data of hotspots (fire position) from Worldview (https://worldview.earthdata.nasa.gov/) and daily data of methane emission from CAMS GFAS (Global Fire Assimilation System) [13, available at https://apps.ecmwf.int/datasets/data/cams-gfas/]. The Global Fire Assimilation System (GFASv1.0) calculates biomass burning emissions by assimilating fire radiative power observations from the MODIS instruments onboard Terra and Aqua satellites (resolution: 0.1×0.1).

The simulation was carried out by WRF-Chem v 4.12 [14]. For the numerical simulation, the domain in the Lambert projection was used, limited horizontally by – 45-74°N and 40-105°E and with the height from the ground to 50 hPa. The number of nodes in the computational domain was 99x104x21 in longitude, latitude, and height, respectively. The horizontal grid spacing was 4 km, a variable time modeling step was used in the range from 30 to 300 s for the meteorological parameters and 6 s for the chemical reactions, the grid step-in height was given by the ETA coordinate taking into account the orographic surface, and increased with increasing height. The height of the lower level was 50 m, and the relief data was set with a resolution of 30".

As the initial meteorological values we used the data of the FNL (NCEP) model [15] with a 6-hour time resolution. Fields of the initial FNL meteorological data were obtained based on GFS data using an increased volume of observational data. The source of anthropogenic emissions HTAP-2 [16] was used to specify the emission sources; methane emissions were supplemented from the EDGAR V.

4.3.2 database [17] with a spatial resolution of 0.1x0.1° and a time resolution of 1 month. The power of the sources was set constant without taking into account the intraday and weekly dynamics of the emissions. The emission sources were specified in the surface layer.

Biogenic emissions were set using the MEGAN2.04 model [18], and emissions from fires were FINN v1.5 [19]. Emissions from swamps were set with constant values using the results of MACC II inverse modeling for 2012 [20]. The initial and boundary conditions for the chemicals were set using the global Mozart4 model for 2013 and the WACCM model for 2020. The parameterizations used in the Wrf-Chem model are: microphysics – Morrison; long-wave radiation – RRTM; shortwave radiation – Dudhia; surface layer – Rev. MM5; surface model – Noah; boundary planetary layer – Yonsei Univ.; cloud parameterization – Grell 3D. The WRF-Chem emission module code has been upgraded to allow methane emissions from fires and bioemissions to be read. In the calculations, the chemical mechanism MOZART-4 [22] was used together with the aerosol mechanism MOZAIC [21]. The chemical block of the model uses 85 substances, 157 reactions, and 39 photochemical ones. The aerosol block allows calculations for 4 size ranges, with median diameters of 0.078125, 0.3125, 1.25, and 5 μm.

3. Results

3.1. The observed change in gas and aerosol compositions, atmospheric circulation features

Figure 1 shows the gas and aerosol concentration in April 2020, the surface temperature measured at the TOR station, and the GHGS blocking conditions. According to Figure 1, two episodes of an increase in the concentration of gases and aerosols for the stations can be distinguished (shown by gray bars in the figure). Let us consider both episodes in detail.

1st event: April 13-15 with a maximum of April 14. Increases in the concentration were characteristic of the suburban area for concentrations of aerosol, as well as NO, NO_2, CO, CO_2. A study of the circulation and temperature features on April 14 demonstrated several points that could help understand the reason for the differences. Both stations were within a single region of atmospheric circulation (PV-Θ, Figure 2a) (the trajectory calculations also confirm this using HYSPLIT, Figure not shown). Both stations were characterized by transfers from the eastern regions of Siberia (north of Irkutsk region). The studied areas were in a baric saddle according to the maps of the 500 hPa geopotential. However, an extremely curious fact is that the temperature difference for the regions in the single circulation zone was 3.4 °C. For the suburban area, the daily average temperature was significantly higher. In this period there were no wildfire areas around both stations. The likely cause of the differences in the gas and aerosol composition may be the mesoscale circulation conditions, as well as the influence of the urban area for the TOR-station or/and the Ob River for the FON-station.

2nd event: April 17-24 with a maximum of April 23. First of all, attention is drawn to the change in the ozone concentration for both stations (The O_3 was almost two times higher than average for 2009-2018 April for the Fonovaya station). A synchronous change is also characteristic of the aerosol concentration. It can be seen that the CO/CO_2 ratio increased for both stations; however, for the episode under consideration it was more significant in the background. For the TOR station, the first episode was more pronounced in an increase in the concentration of CO and CO_2. Besides, we noted that for the case of the second event only for the background conditions there was an increase in NO and NO_2. Moreover, an increase in the SO_2 concentration was also noted. The predominance of the meridional form with the development of high-pressure ridges for the circulation in the middle atmosphere was characterized. The air masses from the southern regions (Kazakhstan) (Figure 2b) are transported throughout the south of Western Siberia. The transport of air masses from the industrial areas of Kazakhstan is confirmed by the calculated background trajectories (Figure 3a). The second important factor characterizing the second episode is a large number of natural fire sources (Figure 3b). The TOR station territory is more subject to smoke from fires.

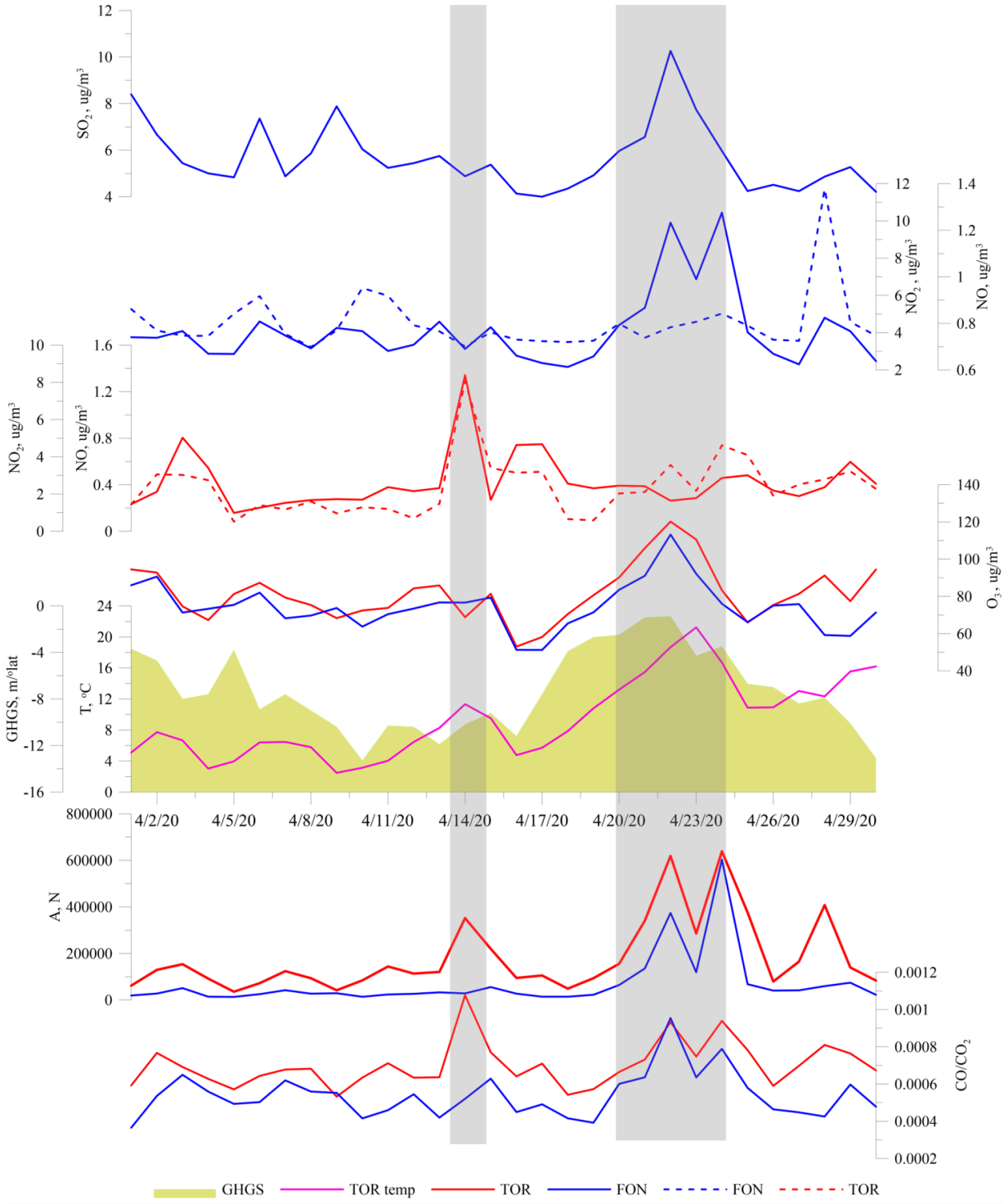

Figure 1. GHGS indexes of blocking, surface temperature (T) for TOR station, gases (CO - carbon oxide, CO_2 - carbon dioxide, O_3 – ozone, SO_2 – sulphur dioxide, NOx – nitrogen oxides), and aerosol (A) (0,25 µm for TOR, 0,30 µm for FON) concentration in April 2020.
Data for FON station:10m level, daily.

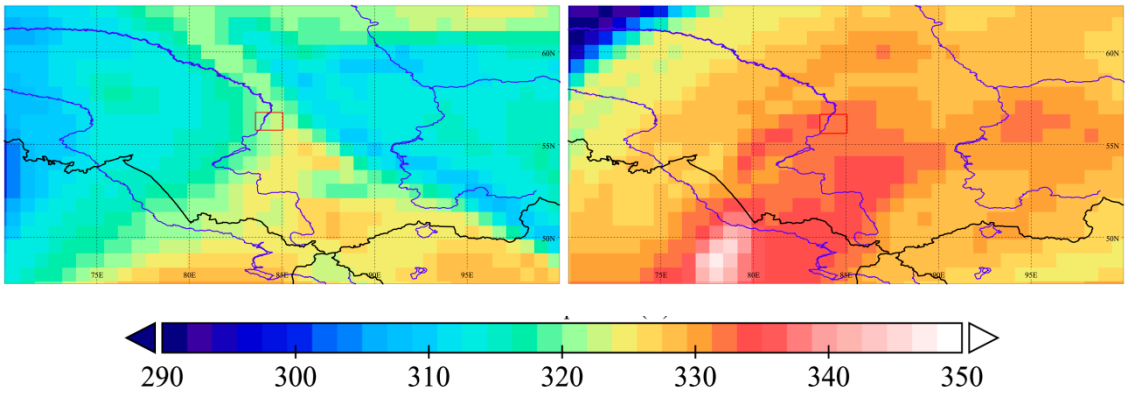

a *b*

Figure 2. PV-Θ (K) on 14 (a) and 24 (b) April 2020. *Area of interest: red rectangle.*

(a)

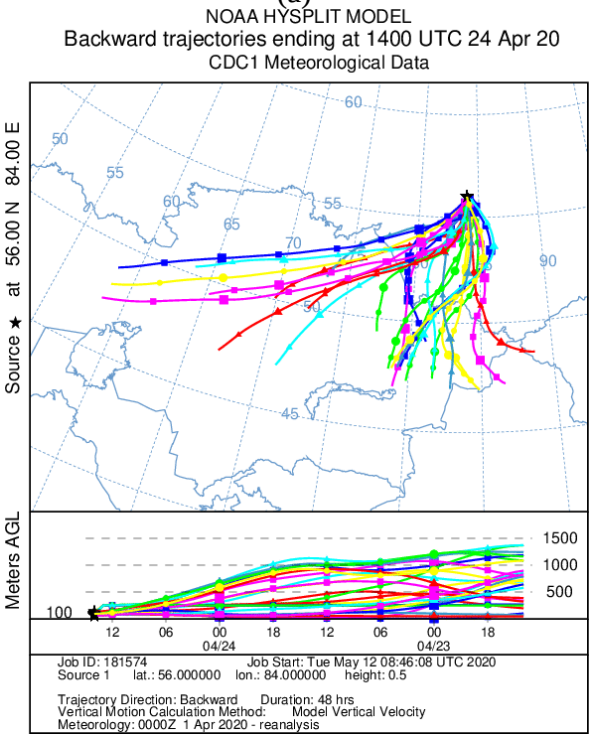

(b)

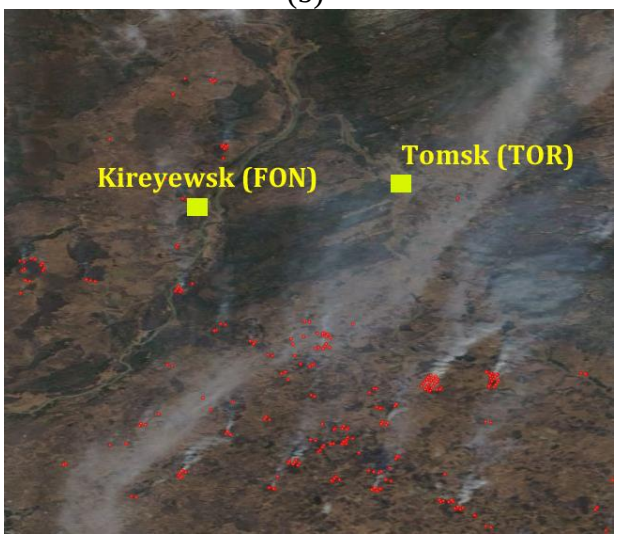

Figure. 3. Backward trajectories of air particles for April 24, 2020 (a), fire hotspots on April 23, 2020, in the southern part of Western Siberia (around the monitoring station) (b).

3.2. Simulation of gas and aerosol composition

Figure 4 shows selective time series of the observed and simulated gas and aerosol composition. To estimate the contribution of emissions from fires to the composition of the atmosphere, two simulation runs were performed. The first run was performed using all emissions (in the figure it is denoted by "all"). For the second run, emissions from fires were turned off (in the figure it is denoted by "abw").

The model reproduces individual elements of changes in the gas and aerosol components (two episodes of increasing gases and aerosols), but it strongly depends on the block "natural fires". It can be seen that for most of the time series in Figure 4 there is no evident increase in the chemical atmospheric composition when the block counts wildfires were turned off. In most cases, the model demonstrated overestimated values or peaks which have not been observed.

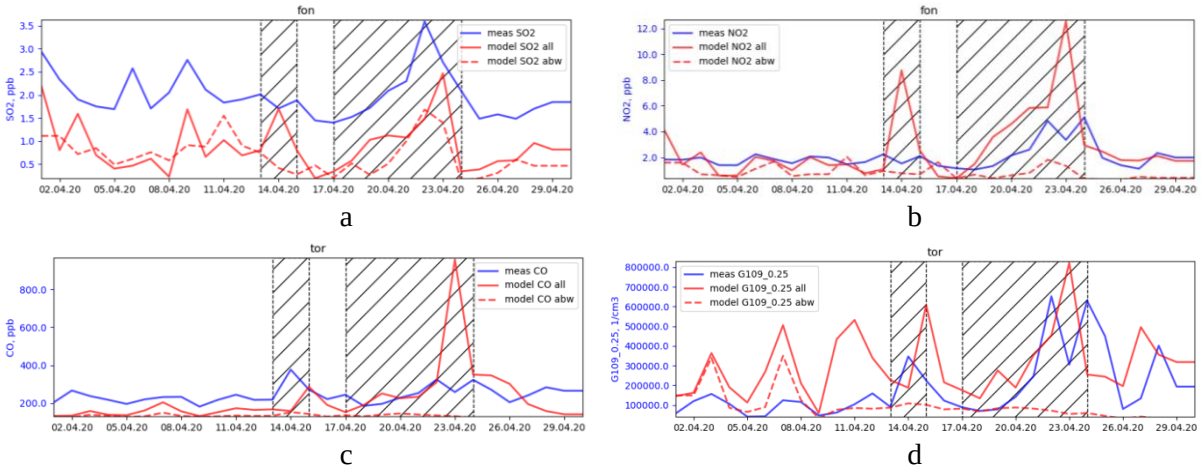

Figure 4. Time series of observed and simulated gas and aerosol composition for FON (a,b) and TOR (b,c) stations.

4. Summary and discussion

The paper presents the result of a comprehensive analysis of the formation of gases and aerosols composition during the anomalously hot April of 2020 in Western Siberia. The analysis of observed changes in the atmospheric composition and simulation with the WRF-Chem model was carried out for suburban (TOR-station) and background (FON-station) areas. Two episodes of increased gases and aerosols were detected: 13-15 April with a peak on 14 (in most part for the TOR station: increased NO, NO_2, CO, CO_2, aerosols) and 17-24 April with a peak on 23 (for both station O_3, aerosol, in most part for the FON station: NO_2, SO_2, CO, and CO_2). The atmospheric circulation for the first episode was characterized by mesoscale differences between the two studied locations (big surface temperature delta, although both stations are in the same region of large-scale transfers). For the second episode, a large scale atmospheric ridge was observed, which caused a transboundary transfer from Northern Kazakhstan and early wildfires.

We can formulate two main hypotheses about the increase in the gas and aerosol composition in the background and suburban conditions in the second episode of April 2020:

1. The role of local mesoscale conditions for the first episode is probably due to the difference between the background and suburban areas. The first episode was not outstanding and most likely was not due to the abnormally warm April. Hence, we have not associated it with anomaly conditions.
2. The role of transfer from the industrial centers of Northern Kazakhstan for the second episode we associated with anomalous circulation conditions. The case under consideration for changes in ozone concentration is similar to that considered previously [23]. The previous paper showed the likelihood of a significant influence of the transfer of additional sources of ozone and its precursors from the southern regions of Kazakhstan for cases of three or more times the increase in the average daily maximum permissible concentration (MPC) of ozone. Therefore, all cases of exceeding three or more times the ozone MPC at the TOR station coincided with an increase in the meridional transport from Kazakhstan and a simultaneous increase in the surface temperature. The case under consideration, in terms of changes in the ozone concentration, surface temperature, and the GHGS index, entirely coincides with those considered in [23].
3. The role of wildfire smoke plumes for the second episode which we associated with the anomaly in circulation in April 2020. Changes in the concentration of CO and CO_2 confirm partially the effect of fires.

For the second episode of the increase in the gas and aerosol composition, it can be necessary to figure out the ratio of different pollution sources (transboundary pollution transport and wildfires fire plume). The influence of long-range pollution transfer is evidenced by an increase in the ozone concentration, similar to earlier cases ([23] where similar cases were discussed). Also, the difference

in the concentration growth for two stations: for example, SO_2, NO_2 – an increase is characteristic only for the background station, where the effects of plumes from fires are less pronounced (Fig. 3b). For suburban conditions, the effect of transboundary transport of SO_2 and NO_2 is not expressed. In the case of the background station, it is more evident to look for a response to the transboundary transfer of pollution. For both stations, the role of wildfires may also be significant. However, the simulation with WRF has demonstrated in most cases only the role of wildfires and, in general, has not demonstrated the noted observed differences between the two episodes. It showed that there is a need to search for more sensitive methods of discovering sources of pollution (especially in case of photochemistry of the atmosphere).

Acknowledgments
This research was supported by the Russian Foundation for Basic Research, grants no. 19-05-50024 "Microparticles in the Atmosphere: Formation and Transformation in the Atmospheric Surface Layer and the Free Troposphere, Radiation Effects and Impact on Public Health." Support for using equipment to measure atmospheric composition (including CCU "Atmosphere") was partially provided by the Ministry of Science and Higher Education of the Russian Federation (budget funds for IAO SB RAS) (state registration number AAAA-A17-117021310142-5).

References

[1] Antokhin P N, Antokhina O Yu, Arshinov M Yu, Belan B D, Davydov D K, Sklyadneva T K, Fofonov A V, Sasakawa M, Machida T 2017 Impact of atmospheric blocking in Western Siberia on the change in methane concentration in the summer period *Atmos. Oceanic Opt.* **30**(5) 393-403 (in Russian with English abstract)
[2] Sitnov S A and Mokhov I I 2018 Anomalies in the Atmospheric Methane Content over Northern Eurasia in the Summer of 2016 *Doklady Earth Sciences* **480** 637–41
[3] Arshinov M *et al* 2018 Station for the comprehensive monitoring of the atmosphere at Fonovaya Observatory, West Siberia: current status and future needs *Proc of 24th International Symposium on Atmospheric and Ocean Optics: Atmospheric Physics*
[4] Davydov D K *et al* 2019 Monitoring of Atmospheric Parameters: 25 Years of the Tropospheric Ozone Research Station of the Institute of Atmospheric Optics, Siberian Branch, Russian Academy of Sciences *Atmos. Oceanic Opt.* **32** 180–92
[5] Dee D P *et al* 2011 The ERA-Interim reanalysis: configuration and performance of the data assimilation system *Quarterly Journal of the Royal Meteorological Society* **137** 553–97
[6] Hersbach H, Bell W, Berrisford P, Horányi A J, M-S Nicolas J, Radu R, Schepers D, Simmons A, Soci C, Dee D 2019 Global reanalysis: goodbye ERA-Interim, hello ERA5. *ECMWF https://www.ecmwf.int/node/19027.*
[7] Kalnay E *et al* 1996 The NCEP/NCAR 40-Year Reanalysis Project *Bulletin of the American Meteorological Society* **77** 437–71
[8] Lejenäs H and Økland H 1983 Characteristics of northern hemisphere blocking as determined from a long time series of observational data *Tellus A* **35**A 350–62
[9] Tibaldi S and Molteni F 1990 On the operational predictability of blocking *Tellus* A **42** 343–65
[10] Barriopedro D, García-Herrera R, Lupo A R and Hernández E 2006 A Climatology of Northern Hemisphere Blocking *Journal of Climate* **19** 1042–63
[11] Antokhina O Y, Antokhin P N, Zorkal'tseva O S and Devyatova E V 2017 Atmospheric blockings in Western Siberia. Part 1. Detection features, objective criteria, and their comparison *Russian Meteorology and Hydrology* **42** 644–52
[12] Masato G, Hoskins B J and Woollings T J 2011 Wave-breaking characteristics of midlatitude blocking *Quarterly Journal of the Royal Meteorological Society* **138** 1285–96
[13] Kaiser J W *et al* 2011 Biomass burning emissions estimated with a global fire assimilation system based on observed fire radiative power *Biogeosciences Discussions* **8** 7339–98
[14] Grell G A, Peckham S E, Schmitz R, Mckeen S A, Frost G, Skamarock W C and Eder B 2005

Fully coupled “online” chemistry within the WRF model *Atmospheric Environment* **39** 6957–75
[15] Commerce S D 2000 National Centers for Environmental Prediction/National Weather Service/NOAA/U., NCEP FNL Operational Model Global Tropospheric Analyses, continuing from July 1999, CISL RDA: NCEP FNL Operational Model Global Tropospheric Analyses, continuing from July 1999, 12 April 2000, https://rda.ucar.edu/datasets/ds083.2/
[16] Janssens-Maenhout G *et al* 2015 HTAP_v2.2: a mosaic of regional and global emission grid maps for 2008 and 2010 to study hemispheric transport of air pollution *Atmospheric Chemistry and Physics* **15** 11411–32
[17] Crippa M *et al* 2018 Gridded emissions of air pollutants for the period 1970–2012 within EDGAR v4.3.2 *Earth System Science Data* **10** 1987–2013
[18] Guenther A, Karl T, Harley P, Wiedinmyer C, Palmer P I and Geron C 2006 Estimates of global terrestrial isoprene emissions using MEGAN (Model of Emissions of Gases and Aerosols from Nature) *Atmospheric Chemistry and Physics* **6** 3181–210
[19] Wiedinmyer C, Akagi S K, Yokelson R J, Emmons L K, Al-Saadi J A, Orlando J J and Soja A J 2011 The Fire Inventory from NCAR (FINN): a high-resolution global model to estimate the emissions from open burning *Geoscientific Model Development* **4** 625–41
[20] Barratt M, MACC-II, ECMWF, 7 Jan 2019<https://www.ecmwf.int/en/research/projects/macc-ii>.
[21] Emmons L K *et al* 2010 Description and evaluation of the Model for Ozone and Related chemical Tracers, version 4 (MOZART-4) *Geoscientific Model Development* **3** 43–67
[22] Zaveri R A, Easter R C, Fast J D and Peters L K 2008 Model for Simulating Aerosol Interactions and Chemistry (MOSAIC) *Journal of Geophysical Research* **113**
[23] Savkin D, Belan B, Antokhina O and Tolmachev G 2017 Dependence of the surface ozone concentration on the air temperature and conditions of atmospheric circulation in Western Siberia in the warm season (May-September) *Proc. Of 23rd International Symposium on Atmospheric and Ocean Optics: Atmospheric Physics*